Published in final edited form as:
Cancer Lett. 2010 June 28; 292(2): 176–185. doi:10.1016/j.canlet.2009.11.023.

Induction of Neuronal Apoptosis Inhibitory Protein Expression in Response to Androgen Deprivation in Prostate Cancer

Helen H.L. Chiu[1], **Theresa M.K. Yong**[1], **Jun Wang**[1], **Yuwei Wang**[2], **Robert L. Vessella**[3], **Takeshi Ueda**[4], **Yu-Zhuo Wang**[2], and **Marianne D. Sadar**[1]

[1]Canada's Michael Smith Genome Sciences Centre, British Columbia Cancer Agency, 675 West 10thAvenue, Vancouver, British Columbia, Canada V5Z 1L3

[2]Department of Cancer Endocrinology, British Columbia Cancer Agency, 675 West 10thAvenue, Vancouver, British Columbia, Canada V5Z 1L3

[3]Department of Urology, University of Washington Medical Center, 1959 N.E. Pacific Street, Seattle, WA 98195

[4]Division of Urology, 666-2 Nitona-cho, Chuo-ku, Chiba Cancer Center, Chiba, Japan, 260-8717

Abstract

A mechanism for survival of prostate cancer cells in an androgen-deprived environment remains elusive. Here, we find that expression of neuronal apoptosis inhibitory protein (NAIP) was significantly increased *in vivo* and *in vitro* in response to androgen deprivation therapy (ADT). Increased expression of NAIP corresponded to increased DNA-binding activity of NF-κB that physically associated to previously uncharacterized κB-like sites in the *NAIP* locus. Importantly, expression of NAIP was significantly increased (p=0.04) in clinical samples of CaP from patients receiving ADT. Expression of NAIP may be associated with enhanced survival of prostate cancer in response to castration.

Keywords

prostate cancer; androgen deprivation; nuclear factor-κB; inhibitors of apoptosis; neuronal apoptosis inhibitory protein

1. INTRODUCTION

Androgen deprivation therapy (ADT) is an effective approach for the treatment of advanced prostate cancer (CaP). This therapy is based on the prostate's dependency on androgen to grow and survive. Unfortunately, despite the initial responsiveness to ADT, the cancer will eventually recur and progress to castration-resistant disease. The molecular mechanisms by which CaP cells survive under androgen-depleted conditions are unknown. Enhanced

Corresponding author: Dr. Marianne D. Sadar, PhD, Canada's Michael Smith Genome Sciences Centre, British Columbia Cancer Agency, 675 West 10th Avenue, Vancouver, British Columbia, Canada V5Z 1L3, Tel: 604-675-8157, Fax: 604-675-8178, msadar@bcgsc.ca.

CONFLICT OF INTEREST

The authors declare that they have no competing interests.

expression of prosurvival proteins is suspected to render some cancer cells less prone to cell death induced by androgen deprivation.

A family of proteins termed inhibitors of apoptosis proteins (IAPs), characterized by the presence of one or more baculoviral IAP repeat domains, is capable of rescuing cells destined for death via the caspase cascade (reviewed by [1]). Eight human IAPs have been identified. These are the neuronal apoptosis inhibitory protein (NAIP/BIRC1), c-IAP1 (BIRC2/HIAP2), c-IAP2 (BIRC3/HIAP1), XIAP (BIRC4), survivin (BIRC5), apollon (BIRC6), livin (BIRC7/KIAP/ML-IAP) and IAP-like protein-2 (BIRC8/ILP-2) [2–8]. IAPs primarily function by restraining the activity of the caspase family. For example, NAIP directly inhibits the cell death effector proteases, caspase-3 and caspase-7 [9] and associates with the initiator caspase, caspase-9 [10]. Thus, it is not surprising that IAPs are deregulated in various malignancies (reviewed in [11]). Elevated expression of IAPs is an early event in the pathogenesis of CaP [12]. Emerging studies imply a role of IAPs in conferring drug-resistance in CaP cells [13–15]. However, the role of IAPs in response to ADT in CaP is understudied.

The cytoprotective properties of IAPs is associated with the nuclear factor (NF)-κB signalling pathway (reviewed by [11, 16]). *c-IAP1*, *c-IAP2*, *XIAP* and *survivin* are NF-κB targets [17–20]. The ubiquitously expressed NF-κB family includes p65/RelA, RelB, c-Rel, p50/p105/NF-κB1 and p52/p100/NF-κB2. Homodimers and heterodimers comprising these subunits regulate a multitude of genes and proteins that are involved in survival and programmed cell death among a variety of biological functions (reviewed in [21]). Although other non-canonical pathways have been described, the activation of NF-κB typically involves phosphorylation of the inhibitor of κB (IκB) by IκB kinase complex. Subsequent ubiquitylation and proteosomal degradation of IκB allows the nuclear translocation, DNA-binding and transcriptional regulation of NF-κB on target genes by binding to the κBsites in the gene loci. The NF-κB signalling pathway is associated with the development and progression of CaP as well as other malignancies (reviewed in [22–24]). Constitutively active NF-κB, p65/p50 heterodimer, has been implicated in the resistance of CaP to apoptosis and disease progression [25–28]. NF-κB can inhibit apoptosis by transcriptional regulation of anti-apoptotic genes [29].

Here, we investigated the effect of androgen deprivation on IAPs and NF-κB in CaP. Since NAIP showed significantly increased expression in response to androgen deprivation, it was the focus of the study. Increased expression of NAIP in response to ADT suggests a potential mechanism by which some CaP cells may acquire enhanced survival.

2. MATERIALS AND METHODS

2.1 Animal models

The LNCaP hollow fiber model was performed in male athymic nude mice as described [30]. Serum PSA was measured using the IMx® Total PSA Assay (Abbott Laboratories). Mice were castrated 7 days after implantation of the fibers. A group of 5 mice were left intact from any major surgical procedure. Two additional groups of mice were included to control for the surgery. For these two groups of control mice, either a mock castration was performed by making the incision without removal of the testicles, or subcutaneous implantation of testosterone pellet (2.5 mg; Innovative Research of America, Sarasota, FL) upon castration. Subcutaneous LNCaP xenografts were prepared with Matrigel in male NOD-SCID mice. Human CaP transplantable tumor lines, PCa1, AB163, AB220M, were derived from advanced CaP and maintained in male NOD-SCID mice [31]. Two pieces of 2 2 1 mm^3 tissue were grafted beneath the renal capsule of adult mice. A set route of administration, dosage and schedule were followed for docetaxel treatment (Sanofi-

Aventis). 14 days after grafting, the mice were divided into two groups: one was administered with docetaxel by intraperitoneal injection (dose of 15 mg/kg) on days 14 and 17. Control mice were given saline as vehicle control. On day 20, mice were euthanized and grafts harvested and examined for take rate and tumor volume. Tissue specimens were snap-frozen in RNAlater® (Ambion, Austin, TX) for gene and protein analyses or fixed in 10% formalin and embedded in paraffin block for pathological examination. The efficacy of docetaxel in xenografts was evaluated by comparing T/C values that were calculated as relative tumor growth of the treated (T) group (median relative volume of the treated) expressed as a percentage to the tumor growth of the control (C) group (median relative volume of the control): $T/C = (T- T_0)/(C-C_0)$[32] All animal procedures were in compliance with the Canadian Council on Animal Care and Institutional Certification.

2.2 RNA extraction and RT-PCR

Total RNA was extracted from *in vitro* cells using Trizol® Reagent (Invitrogen). For xenografts, cubes of 2–5 mg of tumor tissue were homogenized and total RNA was isolated using the RNA Easy Micro Kit (Qiagen). Reverse transcription (RT-PCR) and real-time quantitative PCR (qPCR) were performed separately in triplicates for each biological sample. Poly$(A)^+$ RNA was reverse transcribed using oligo(dT) and the SuperScript III First-Strand Synthesis System. qPCR was performed with Platinum® SYBR® Green qPCR SuperMix-UDG with ROX (Invitrogen). Primers were designed to generate PCR products of <200 bp (Suppl. Table 1). Results were reviewed using the SDS 2.2 software (Applied Biosystems). Levels of expression were normalized to levels of GAPDH mRNA to give the mean normalized expression (MNE). MNE = CT value of reference gene $^{(\text{primer efficiency})}$/CT value of target gene $^{(\text{primer efficiency})}$.

2.3 Protein extracts and Western blot analyses

Protein extracts were prepared from cells lysed in hypotonic buffer [33]. The supernatant (cytosolic fraction) was removed and stored. The pellet was resuspended in high salt buffer to extract nuclear proteins. Protein concentration was quantified by Bradford assay (Bio-Rad). Western blot analysis of NAIP employed cytosolic extracts (60μg protein) with anti-human NAIP antibody (ab25968, Abcam). The membranes were stripped with Restore Western Blot Stripping Buffer (Pierce) and reprobed with monoclonal anti-β-actin (ab8226, Abcam).

2.4 Electrophoretic mobility shift assay (EMSA)

Double-stranded oligonucleotides (22 base pairs), NF-κB consensus oligonucleotide (5’-AGTTGAGGGGACTTTCCCAGGC-3’), NF-κB mutant oligonucleotide (5’-AGTTGAGGCGACTTTCCCAGGC-3’), κB-like-1 consensus oligonucleotide (5’-ATTCAGGGGGATTTACAGTCAT-3’), κB-like-1 mutant oligonucleotide (5’-ATTCAGGGCGATTTACAGTCAT-3’), κB-like-2 consensus oligonucleotide (5’-AGGATGGGGGCTATCCCCTGAA-3’), κB-like-2 mutant oligonucleotide (5’-AGGATGGGCGCTATCCCCTGAA-3’), κB-like-3 consensus oligonucleotide (5’-ATAGAAGGTAATTTCCCAGGCT-3’), κB-like-3 mutant oligonucleotide (5’-ATAGAAGCTAATTTCCCAGGCT-3’) were radiolabelled and used for EMSA. Supershift assays preincubated nuclear extracts with anti-p65 antibody or anti-p50 antibody. Competition binding assays preincubated nuclear extracts with 250-fold excess unlabeled oligonucleotides. The density of the shifted band that corresponded to a protein-DNA complex was analyzed using ImageQuant® 5.2 (GE Healthcare).

2.5 In-vitro androgen deprivation

LNCaP cells were incubated in RPMI 1640 supplemented with 5% charcoal-stripped bovine serum with 10nM DHT for 20h. The cells were washed with serum-free medium (SFM) to remove residual DHT. For *in-vitro* androgen deprivation, the media was replaced with fresh SFM and the cells cultured in the androgen-deprived environment. Control cells were maintained in SFM supplemented with 10 nM DHT after washing. Cells were harvested after another 27h of incubation.

2.6 NF-κB luciferase reporter activity assay

LNCaP cells were transfected with a NF-κB luciferase reporter vector (Panomics) containing six tandem copies of the consensus κB site using Lipofectin reagent (Invitrogen). After 24h, cells were treated for an additional 24h before harvesting and measurement of luciferase activity normalized to protein concentration.

2.7 Chromatin immunoprecipitation (ChIP)

After plating cells, the media was replaced with SFM for an additional 24 h. Cells were treated with SFM supplemented with BSA (1 mg/ml) in the presence or absence of TNF-α (10 ng/ml) for 30 min. The proteins were cross-linked with formaldehyde, washed, pelleted, and lysed. The cell extract was sonicated to give an average length of 200–800 bp of sheared DNA fragments. The antibody-protein-DNA complex was precipitated by incubating with nProtein A-Sepharose beads (Amersham Biosciences, Buckinghamshire, UK). The beads were pelleted, washed and the protein-DNA complex eluted from the beads. The cross-linking of the DNA protein complex was reversed and the DNA was recovered and purified. The promoter and intronic regions of *NAIP* were amplified using qPCR with primers (Suppl. Table 2). The thermal cycling conditions were 50ºC for 2min, 95ºC for 2min, followed by 45 cycles of 30s at 95ºC, 30s at 55ºC and 30s at 72ºC. Percentage input was calculated from dividing the arbitrary qPCR numbers obtained from each sample by that of the input.

2.8 Immunohistochemistry

Processed tissue sections of xenografts were immunostained with anti-human NAIP antibody (R&D Systems). The VECTASTAIN® ABC Kit (Vector Laboratories) was used for detection. Peroxidase activity was localized with 3,3'-diaminobenzidin, and the sections were counterstained with hematoxyline before dehydration and mounting. For TUNEL staining, the ApopTag® Fluorescein *In Situ* Apoptosis Detection Kit (Chemicon International) was used followed by counterstaining with propidium iodide (PI).

2.9 Clinical samples

Androgen-dependent CaP specimens were from patients who had undergone radical prostatectomy and were obtained through co-author TU. Clinical samples of men receiving ADT were obtained from the Prostate Cancer Rapid Autopsy Program at the University of Washington through co-author RLV. Informed consent was obtained from each patient in compliance with ethical and scientific standards (UBC/BCCA Research Ethics Board).

3. RESULTS

3.1 ADT increases levels of NAIP transcript *in vivo*

The LNCaP hollow fiber model restricts contamination of cells within the fiber by host cells [30] and was employed to investigate the levels of expression of the IAPs genes, *NAIP*, *c-IAP1*, *XIAP* and *survivin* in response to ADT. Total RNA was isolated from LNCaP cells retrieved before castration (7 days after implantation) and 10 days after castration (17 days

after implantation). The levels of mRNA for *NAIP*, *c-IAP1*, *XIAP* and *survivin*, were measured by qPCR (Fig. 1). Levels of *PSA* mRNA were decreased in response to castration as expected and consistent with clinical representation [34, 35]. Levels of mRNA for *c-IAP1*, *XIAP* were not significantly changed in response to ADT at this time point. However, both *survivin* (decreased, $p<0.01$) and *NAIP* (increased, $p<0.01$) showed significant changes in levels of mRNA in response to ADT.

3.2 ADT increases NF-κB activity

NF-κB may promote anti-apoptotic properties via transcriptional regulation of survival genes such as *c-IAP2* [36] and *survivin* [17]. This prompted us to explore levels and biological activity of NF-κB in CaP in response to ADT using *in vivo* samples. Serum PSA levels dropped by an average of 57 % by 10 days after castration of mice implanted with fibers containing LNCaP cells (Fig. 2A). Nuclear levels of NF-κB (p65 and p50) proteins were unchanged in extracts obtained from the LNCaP hollow fiber model before and after castration as measured by western blot analysis (Fig. 2B). Quantification of protein bands obtained from the replicate experiments are shown in Suppl. Fig. 1A.

To determine the effect of ADT on the DNA-binding activity of NF-κB, aliquots of nuclear extracts (20 μg protein in each lane) prepared from the LNCaP hollow fiber model before castration and after castration were analysed using EMSA (Fig 2C). Nuclear extracts from cells treated with tumor necrosis factor-α (TNF-α) were included as a positive control and showed strong bands corresponding to p65/p50 and p50/p50 complex formation with DNA (compare lanes 2 and 3). The specificity of the shifted bands corresponding to the different NF-κB DNA complexes was confirmed by supershift assay in the presence of anti-p65 or anti-p50 antibody (lanes 4 and 5) or competition assay in the presence of excess, non-labelled, consensus (lane 6) or mutant oligonucleotide probes (lane 7). The band corresponding to p65/p50 in lane 2 was shifted with an antibody to p65 (lane 4), although the new band formed by the antibody-NF-κB DNA complex was weak (upper “SS) which may reflect reduced affinity that can occur with antibody complexes. NF-κB DNA-binding activity was elevated substantially in response to castration (compare lane 9 to lane 8). The densities of the bands corresponding to the NF-κB (p65/p50)-DNA complexes were quantified and the average fold-induction was over 2.5-fold relative to the pre-castrate levels from biological triplicates (Fig. 2C).

Three groups of procedural control mice [i.e. intact, mock castration (Cx), castration with the addition of testosterone pellet (Cx + T)] were maintained throughout the same length of time as the hollow fiber model experiment with castrated mice. Likewise with mice subjected to castration, cells were collected at the relative times to assess for the expression and DNA-binding activity of NF-κB. The results are displayed in parallel with the data from mice subjected to castration (Fig. 2D). No significant change in serum PSA levels in intact mice and mock Cx mice was observed in 7 days and 17 days after implantation of fibers except for Cx + T mice. Nuclear extracts prepared from samples obtained at 7 days and 17 days after implantation from intact animals had similar NF-κB expression and DNA-binding activity (Suppl. Fig. 1B). This suggests that the length of time in the fiber had no appreciable effect on NF-κB DNA-binding activity. Similarly, nuclear extracts prepared from samples obtained from mock-castrated animals, or castrated mice supplemented with testosterone also had no difference in NF-κB expression and DNA-binding activity (Suppl. Fig. 1B). Thus, the results from these *in vivo* procedural controls confirm that the results obtained from the castrated mice were not due to artifacts from the invasive surgical procedures performed on the hosts.

3.3 Androgen alters transcriptional activity of NF-κB and expression of NAIP

In the presence of androgen, there is crosstalk between androgen receptor (AR) and NF-κB [37, 38]. To test if androgen had a direct effect on NF-κB activity in our model, the transcriptional activity of NF-κB was evaluated using a luciferase reporter gene construct containing six κB sites. Treatment of LNCaP cells, that express AR, with TNF-α (positive control) strongly induced the activity of this reporter indicating increased NF-κB transcriptional activity (Fig 3A). Treatment of LNCaP cells with synthetic androgen R1881 significantly decreased NF-κB activity as compared to the vehicle control. Thus, androgen inhibited the transcriptional activity of NF-κB.

To test whether the *in vivo* increased levels of *NAIP* mRNA were due to reduced androgen, total RNA was isolated from androgen deprived LNCaP cells maintained *in vitro*. The expression of *PSA* (control for androgen deprivation) and *NAIP* were evaluated by qPCR. Levels of *PSA* mRNA were significantly decreased, as expected, while levels of *NAIP* mRNA were significantly increased ($p<0.01$) in the cells subjected to androgen deprivation (Fig. 3B).

Consistent with increased levels of NAIP mRNA in response to ADT, levels of NAIP protein was also increased with castration as compared to levels in xenografts from non-castrated hosts (Fig. 3C). The increased levels of NAIP protein was localized near the periphery of the tumor tissue near blood vessels. The heterogeneity of NAIP staining could possibly be attributed to macrophages residing in these tissues [39]. Therefore, levels of NAIP protein were also measured by Western blot analysis using extracts of LNCaP cells harvested from the hollow fiber model that restricts infiltration of host cells. Levels of NAIP protein, at approximately 160-kDa, were consistently elevated in cells obtained from animal hosts (n=3) subsequent to castration as compared to levels from non-castrated hosts (Fig. 3D). The increased levels of NAIP protein were consistent with the increased levels of NAIP transcript in CaP cells in response to ADT. Together, the data suggest that ADT increases the expression of NAIP in CaP.

3.4 Recruitment of NF-κB to the NAIP locus

Increased NAIP expression followed the same trend observed for NF-κB DNA-binding activity in response to androgen deprivation and suggests a possible association between NAIP and NF-κB. Consistent with this observation, there has been speculation by others that the expression of *NAIP* may be directly regulated by NF-κB [40, 41]. However biological evidence has yet to be provided. The human *NAIP* locus [GeneBank Accession No. U19251] [42] was therefore examined for putative κB sites (GGGRNNYYCC [R=purine, N=any base, Y=pyrimidine]) using ConSite [http://asp.ii.uib.no:8090/cgi-bin/CONSITE/consite/] [43] with an 80% cutoff. Initial screening with ConSite revealed two κB-like sites in the promoter region and one κB-like site within the second intron of *NAIP* that were highly homologous to the consensus κB site (Table 1). To test NF-κB binding on these κB-like sequences, EMSA was employed using custom oligonucleotide probes that contain the κB-like sites and nuclear extracts from *in vitro* and *in vivo* (i.e. from the hollow fiber model) LNCaP cells. Supershift and competition assays were performed to confirm the specificity of the NF-κB-DNA complexes. Nuclear extracts from cells treated with TNF- were used as a robust positive control and produced NF-κB complexes on all 3 κB-like sites (Fig. 4A). NF-κB DNA-binding activity in nuclear extracts from *in vivo* samples demonstrated enhanced DNA-binding activity in samples from castrated hosts on all κB-like sites with κB-like site-3> κB-like site-1> κB-like site-2. NF-κB complexes binding on these κB-like sites suggested that the expression of NAIP may be transcriptionally regulated by NF-κB binding to these sites located within the promoter and intronic regions in the gene locus.

The physiological relevance of NF-κB binding on these κB-like sites in the promoter and intronic regions of *NAIP*, was validated by ChIP assays in cells stimulated with TNF-α. Subsequent to cross-linking of protein-DNA complexes, immunoprecipitations were performed using an antibody specific for p65. Primers specific for the κB-like sites on the promoter and intronic regions of *NAIP* were used to amplify the immunoprecipitated DNA using qPCR. Immunoprecipitation of sonicated nuclear extracts with rabbit IgG was performed in place of anti-p65 antibody as controls for no antibody. The recruitment of p65 was enhanced on all κB-like sites in the *NAIP* locus in response to TNF-α as compared to the recruitment in the vehicle control (Fig. 4B). Recruitment on κB-like-3 site that is located within the second intronic region demonstrated statistically significant increase in physical association by ChIP which was consistent with the 1.9-fold increase in DNA-binding activity on κB-like-3 site obtained using EMSA ($p \leq 0.05$) Suppl. Fig. 2)

3.5 Elevated NAIP expression in chemoresistant tumors with reduced apoptosis

Docetaxel is an effective chemotherapy agent approved for castration-resistant CaP [44]. A transplantable xenograft model originally derived from human CaP [31] was employed to test whether endogenous levels of NAIP expression correlated to response to docetaxel and apoptosis. Each of these transplantable xenografts had 100% take-rate and similar doubling times of 3–4 days. Animals were treated with docetaxel as well as control injection of carrier (i.e. saline). Total RNA was extracted from the xenografts and subjected to qPCR. The level of NAIP mRNA was significantly higher in PCa1 xenografts than AB163 or AB220M xenografts regardless of exposure to docetaxel (Fig. 5A). To test the susceptibility to docetaxel treatment in these different xenografts, tumour volume in control and treated mice was evaluated at the endpoint. The tumour volume of PCa1 was not significantly altered, while AB163 and AB220M with low levels of endogenous NAIP, regressed significantly in response to docetaxel (Fig. 5B). These transplantable tumor lines innately show a different responsiveness to docetaxel. The efficacy of docetaxel in different xenografts was compared by treatment to control (T/C value) calculation. Comparing with the T/C values, the efficacy of docetaxel was the least in PCa1 (53.6%) followed by AB220M (33.90%) and AB163 (5.48%). Both AB163 and AB220M xenografts can be assessed as sensitive lines to docetaxel, since the criterion for efficiency for the T/C ratio is ≤42% according to National Cancer Institute standards [32]. To further examine the resistance to apoptosis in these xenografts in response to docetaxel, the TUNEL assay was employed to measure the apoptotic cells in these tumours. PCa1 xenografts were not significantly susceptible to docetaxel as compared to AB163 and AB220M which demonstrated significant increase in apoptosis (Fig. 5C). TUNEL staining images highlight the contrast in number of apoptotic cells observed in PCa1 versus AB163 or AB220M (Fig. 5D). Results from this transplantable CaP xenograft model showed that expression of NAIP is positively correlated with the inhibition of both tumor regression and apoptosis in response to docetaxel.

3.6 Expression of NAIP in clinical samples

Levels of PSA and NAIP mRNAs were examined in CaP from men who were treated with or without ADT. Tissue levels of PSA mRNA was significantly reduced in patients (n=12) that received ADT (p=0.0056) (Fig. 6A), while levels of NAIP mRNA in these same samples were significantly elevated (p=0.0403) as compared to the levels measured in patients (n=6) without ADT (Fig. 6B). These data are consistent with both *in vitro* and *in vivo* results that ADT increases expression of NAIP.

4. DISCUSSION

Progression of CaP to castration-resistance may involve outgrowth of CaP cells in response to ADT with distinct molecular properties that are resistant to apoptosis. Accumulating

evidence support the role of IAPs in CaP as anti-apoptotic regulators (reviewed in [45]). Here we investigated expression of NAIP in CaP in response to ADT and revealed the following: 1) levels of NAIP mRNA and protein increased in vivo in response to ADT; 2) NF-κB DNA-binding and transcriptional activities increased in response ADT; 3) NF-κB binds to two κB-like sites in the promoter region and one κB-like site within the second intron of the *NAIP* locus; 4) high levels of endogenous expression of NAIP correlated to resistance to apoptosis by docetaxel in CaP xenografts; and 5) clinical samples of CaP with ADT have significantly higher expression of NAIP ($p=0.04$) compared to CaP with no ADT.

Examination of changes in expression of several of the IAP genes revealed that *NAIP* was significantly increased in response to ADT *in vivo* and in clinical CaP specimens from men treated with ADT. The expression of *survivin* was significantly decreased, while the expression of *c-IAP1* and *XIAP* were not significantly altered in the hollow fiber model. *Survivin* is predominantly expressed in the G2/M phase of the cell cycle and promotes mitosis in rapidly dividing cells (reviewed in [46]). ADT initially results in decreased proliferation in LNCaP hollow fiber model [30]. Decreased mRNA levels of *survivin* in this *in vivo* model in response to castration of the hosts may reflect reduced proliferation. Consistent with the data presented here, down-regulation of *survivin* was reported in LNCaP cells maintained in androgen-deprived conditions *in vitro* [47].

Survivin, c-IAP1 and *XIAP* are all transcriptionally regulated by NF-κB [18, 19] and here we provide evidence that the NAIP locus contains functional NF-κB binding sites. However, we did not observe significant increases in expression of all of these genes at 10 days after castration in spite of the increased NF-κB DNA-binding activity. These gene-specific differences may be due to the subtle changes in NF-κB activity demonstrated at the designated time in response to ADT or differences in the kinetics of individual genes. The expression of these genes might require different factor(s) which facilitate the NF-κB signaling and the transcriptional regulation may vary depending on the cellular context and experimental conditions. Collecting *in vivo* samples from additional times after castration may help to address these unknowns by providing a comprehensive profile of NF-κB activity and IAPs expression in response to ADT.

NAIP is the founding member of the family of human IAPs. Deficiency of NAIP from deletions of a gene region is primarily associated with the most severe phenotypes of a hereditary neurodegenerative disorder, spinal muscular atrophy (SMA), due to loss of its neuroprotective activity in motor neurons in the spinal cord [8]. Expression of NAIP in tissues that are not exclusively neuronal and not directly associated with SMA suggests functions beyond its neuronal context [39, 48]. NAIP protects mammalian cells from apoptosis induced by a variety of stimuli [6]. Although no study has been specifically performed in cancer cells, extrapolating the function of NAIP in benign cells would strongly suggest NAIP would also protect cancer cells from apoptosis. Consistent with this role, we observed a correlation of overall sensitivity and reduced apoptosis in response to docetaxel in CaP tissue that expresses elevated levels of NAIP. The absence of strict correlation of sensitivity to docetaxel in tumor lines AB163 and AB220M, that had extremely low levels of NAIP mRNA compared to PCa1, may be attributed to the contribution of other molecular mechanisms when NAIP is poorly expressed. The presence of a central nucleotide binding oligomerization domain and a carboxyl-terminal leucine-rich repeat domain might enable NAIP to promote additional cytoprotection and other functions unique from other IAP members [10]. However, the events regulating NAIP are largely unknown. To begin to address this void, we observed for the first time a link between NF-κB activity and NAIP expression. ADT increased levels of NAIP mRNA and NF-κB DNA-binding activity, and the complementary experiment showed that the presence of androgen inhibited NF-κB activity. The reduction in NF-κB transcriptional activity in the presence of androgen as

demonstrated by the NF-κB luciferase reporter assay suggests that the differential NF-κB DNA-binding activity evident from *in vivo* LNCaP cells corresponded to the androgen levels in the microenvironment of the CaP cells. This means that when a host bearing CaP cells is castrated, an increase in NF-κB DNA-binding activity should be observed. Curiously, nuclear levels of NF-κB did not correlate to its binding activity in extracts prepared from samples maintained *in vivo* in response to castration of the hosts. Thus, NF-κB activity *in vivo* may be modulated by post-translational modification of the NF-κB subunits, such as phosphorylation and acetylation status of the NF-κB subunits (reviewed in [49]). In cell culture, crosstalk between AR and p65 have been shown to mutually repress the transactivation activity of each protein [37, 38]. Consistent with those studies, here transactivation of a NF-κB luciferase reporter construct yielded comparable inhibition in the presence of androgen similar to that used previously [38] in LNCaP cells with endogenous AR.

Elevated levels of NAIP that correlated with increased NF-κB binding activity shown here are consistent with decreased levels of NAIP mRNA in human hepatic cancer cells treated with dehydroxymethylepoxyquinomicin, an NF-κB inhibitor [40] and increased NAIP expression in leukemia cells with constitutive activation of NF-κB [41]. Together these data support that NAIP may be transcriptionally regulated by NF-κB. Here, the application of EMSA reveals NF-κB DNA-binding to 3 previously uncharacterized NF-κB regulatory binding elements in the *NAIP* promoter and intronic regions. ChIP experiments validated significantly increased NF-κB interaction *in situ* on the regulatory element in the second intron. Although these ChIP experiments did not show statistically significant increases in NF-κB interaction on the other κB-like sites in the promoter region, they may still be functional κB-like sites with possibly lower affinity requiring further optimization with a different set of experimental conditions. *NAIP* expression may be regulated by multiple factors including PAX2 [50], a developmental transcription factor and Brn-2 [51], a POU domain transcription factor. However, the binding of PAX2 and Brn-2 to their respective putative regulatory elements on the *NAIP* locus was only demonstrated by EMSA, an *in vitro* assay. Thus, the binding *in situ* has yet to be confirmed using methods such as ChIP as used here. Differences in cofactors involved in the transcriptional complexes under different cellular conditions may be important for regulation of expression of NAIP and putative regulatory elements of other transcription factors are yet to be validated [51]. Our findings demonstrate that NF-κB can regulate the transcription of the *NAIP* gene through *cis*-regulatory elements that resemble the NF-κB consensus binding motif. Intriguingly, the κB-like-3 site which demonstrated the significant increase in binding upon TNF-α stimulation lies 5' upstream and in close proximity to the constitutive transcription start site within the non-long-terminal-repeat promoter [48]. The resulting transcript would yield the same protein product as the commonly-cited transcript [42].

In summary, this first report on investigation of NAIP in CaP reveals elevated expression of NAIP in response to ADT and a link between NF-κB activity and expression of NAIP potentially involving functional NF-κB binding sites in the promoter and intronic regions of the *NAIP* gene. The clinical relevance of elevated expression of NAIP is supported by the profile expression of NAIP in CaP patients with ADT. Together with observations from other groups, the cumulative data suggest future studies that entail deciphering the specific function of NAIP in CaP progression to castration-resistant disease and prognostic value to predict response to chemotherapy are warranted.

Supplementary Material

Refer to Web version on PubMed Central for supplementary material.

Acknowledgments

We thank Nasrin R. Mawji, Rebecca Wu, Gang Wang and Tammy Romanuik for their technical assistance.

GRANT SUPPORT

This research was supported by funding from NIH R01 CA105304 (to M.D.S.).

References

1. Liston P, Fong WG, Korneluk RG. The inhibitors of apoptosis: there is more to life than Bcl2. Oncogene. 2003; 22:8568–8580. [PubMed: 14634619]
2. Chen Z, Naito M, Hori S, Mashima T, Yamori T, Tsuruo T. A human IAP-family gene, apollon, expressed in human brain cancer cells. Biochem Biophys Res Commun. 1999; 264:847–854. [PubMed: 10544019]
3. Vucic D, Stennicke HR, Pisabarro MT, Salvesen GS, Dixit VM. ML-IAP, a novel inhibitor of apoptosis that is preferentially expressed in human melanomas. Curr Biol. 2000; 10:1359–1366. [PubMed: 11084335]
4. Rothe M, Pan MG, Henzel WJ, Ayres TM, Goeddel DV. The TNFR2-TRAF signaling complex contains two novel proteins related to baculoviral inhibitor of apoptosis proteins. Cell. 1995; 83:1243–1252. [PubMed: 8548810]
5. Ambrosini G, Adida C, Altieri DC. A novel anti-apoptosis gene, survivin, expressed in cancer and lymphoma. Nat Med. 1997; 3:917–921. [PubMed: 9256286]
6. Liston P, Roy N, Tamai K, Lefebvre C, Baird S, Cherton-Horvat G, Farahani R, McLean M, Ikeda JE, MacKenzie A, Korneluk RG. Suppression of apoptosis in mammalian cells by NAIP and a related family of IAP genes. Nature. 1996; 379:349–353. [PubMed: 8552191]
7. Richter BW, Mir SS, Eiben LJ, Lewis J, Reffey SB, Frattini A, Tian L, Frank S, Youle RJ, Nelson DL, Notarangelo LD, Vezzoni P, Fearnhead HO, Duckett CS. Molecular cloning of ILP-2, a novel member of the inhibitor of apoptosis protein family. Mol Cell Biol. 2001; 21:4292–4301. [PubMed: 11390657]
8. Roy N, Mahadevan MS, McLean M, Shutler G, Yaraghi Z, Farahani R, Baird S, Besner-Johnston A, Lefebvre C, Kang X, et al. The gene for neuronal apoptosis inhibitory protein is partially deleted in individuals with spinal muscular atrophy. Cell. 1995; 80:167–178. [PubMed: 7813013]
9. Maier JK, Lahoua Z, Gendron NH, Fetni R, Johnston A, Davoodi J, Rasper D, Roy S, Slack RS, Nicholson DW, MacKenzie AE. The neuronal apoptosis inhibitory protein is a direct inhibitor of caspases 3 and 7. J Neurosci. 2002; 22:2035–2043. [PubMed: 11896143]
10. Davoodi J, Lin L, Kelly J, Liston P, MacKenzie AE. Neuronal apoptosis-inhibitory protein does not interact with Smac and requires ATP to bind caspase-9. J Biol Chem. 2004; 279:40622–40628. [PubMed: 15280366]
11. Hunter AM, Lacasse EC, Korneluk RG. The inhibitors of apoptosis (IAPs) as cancer targets. Apoptosis. 2007; 12:1543–1568. [PubMed: 17573556]
12. Krajewska M, Krajewski S, Banares S, Huang X, Turner B, Bubendorf L, Kallioniemi OP, Shabaik A, Vitiello A, Peehl D, Gao GJ, Reed JC. Elevated expression of inhibitor of apoptosis proteins in prostate cancer. Clin Cancer Res. 2003; 9:4914–4925. [PubMed: 14581366]
13. Tirro E, Consoli ML, Massimino M, Manzella L, Frasca F, Sciacca L, Vicari L, Stassi G, Messina L, Messina A, Vigneri P. Altered expression of c-IAP1, survivin, and Smac contributes to chemotherapy resistance in thyroid cancer cells. Cancer Res. 2006; 66:4263–4272. [PubMed: 16618750]
14. Zhang M, Latham DE, Delaney MA, Chakravarti A. Survivin mediates resistance to antiandrogen therapy in prostate cancer. Oncogene. 2005; 24:2474–2482. [PubMed: 15735703]
15. Nomura T, Yamasaki M, Nomura Y, Mimata H. Expression of the inhibitors of apoptosis proteins in cisplatin-resistant prostate cancer cells. Oncol Rep. 2005; 14:993–997. [PubMed: 16142363]
16. LaCasse EC, Baird S, Korneluk RG, MacKenzie AE. The inhibitors of apoptosis (IAPs) and their emerging role in cancer. Oncogene. 1998; 17:3247–3259. [PubMed: 9916987]

17. Kawakami H, Tomita M, Matsuda T, Ohta T, Tanaka Y, Fujii M, Hatano M, Tokuhisa T, Mori N. Transcriptional activation of survivin through the NF-kappaB pathway by human T-cell leukemia virus type I tax. Int J Cancer. 2005; 115:967–974. [PubMed: 15729715]
18. Stehlik C, de Martin R, Kumabashiri I, Schmid JA, Binder BR, Lipp J. Nuclear factor (NF)-kappaB-regulated X-chromosome-linked iap gene expression protects endothelial cells from tumor necrosis factor alpha-induced apoptosis. J Exp Med. 1998; 188:211–216. [PubMed: 9653098]
19. Wang CY, Mayo MW, Korneluk RG, Goeddel DV, Baldwin AS Jr. NF-kappaB antiapoptosis: induction of TRAF1 and TRAF2 and c-IAP1 and c-IAP2 to suppress caspase-8 activation. Science. 1998; 281:1680–1683. [PubMed: 9733516]
20. Chu ZL, McKinsey TA, Liu L, Gentry JJ, Malim MH, Ballard DW. Suppression of tumor necrosis factor-induced cell death by inhibitor of apoptosis c-IAP2 is under NF-kappaB control. Proc Natl Acad Sci USA. 1997; 94:10057–10062. [PubMed: 9294162]
21. Dutta J, Fan Y, Gupta N, Fan G, Gelinas C. Current insights into the regulation of programmed cell death by NF-kappaB. Oncogene. 2006; 25:6800–6816. [PubMed: 17072329]
22. Courtois G, Gilmore TD. Mutations in the NF-kappaB signaling pathway: implications for human disease. Oncogene. 2006; 25:6831–6843. [PubMed: 17072331]
23. Karin M. Nuclear factor-kappaB in cancer development and progression. Nature. 2006; 441:431–436. [PubMed: 16724054]
24. Suh J, Rabson AB. NF-kappaB activation in human prostate cancer: important mediator or epiphenomenon? J Cell Biochem. 2004; 91:100–117. [PubMed: 14689584]
25. Sweeney C, Li L, Shanmugam R, Bhat-Nakshatri P, Jayaprakasan V, Baldridge LA, Gardner T, Smith M, Nakshatri H, Cheng L. Nuclear factor-kappaB is constitutively activated in prostate cancer in vitro and is overexpressed in prostatic intraepithelial neoplasia and adenocarcinoma of the prostate. Clin Cancer Res. 2004; 10:5501–5507. [PubMed: 15328189]
26. Shukla S, Gupta S. Suppression of constitutive and tumor necrosis factor alpha-induced nuclear factor (NF)-kappaB activation and induction of apoptosis by apigenin in human prostate carcinoma PC-3 cells: correlation with down-regulation of NF-kappaB-responsive genes. Clin Cancer Res. 2004; 10:3169–3178. [PubMed: 15131058]
27. Yemelyanov A, Gasparian A, Lindholm P, Dang L, Pierce JW, Kisseljov F, Karseladze A, Budunova I. Effects of IKK inhibitor PS1145 on NF-kappaB function, proliferation, apoptosis and invasion activity in prostate carcinoma cells. Oncogene. 2006; 25:387–398. [PubMed: 16170348]
28. Huerta-Yepez S, Vega M, Garban H, Bonavida B. Involvement of the TNF-alpha autocrine-paracrine loop, via NF-kappaB and YY1, in the regulation of tumor cell resistance to Fas-induced apoptosis. Clin Immunol. 2006; 120:297–309. [PubMed: 16784892]
29. Kucharczak J, Simmons MJ, Fan Y, Gelinas C. To be, or not to be: NF-kappaB is the answer--role of Rel/NF-kappaB in the regulation of apoptosis. Oncogene. 2003; 22:8961–8982. [PubMed: 14663476]
30. Sadar MD, Akopian VA, Beraldi E. Characterization of a new in vivo hollow fiber model for the study of progression of prostate cancer to androgen independence. Mol Cancer Ther. 2002; 1:629–637. [PubMed: 12479223]
31. Wang Y, Xue H, Cutz JC, Bayani J, Mawji NR, Chen WG, Goetz LJ, Hayward SW, Sadar MD, Gilks CB, Gout PW, Squire JA, Cunha GR, Wang YZ. An orthotopic metastatic prostate cancer model in SCID mice via grafting of a transplantable human prostate tumor line. Lab Invest. 2005; 85:1392–1404. [PubMed: 16155594]
32. Bissery MC, Guenard D, Gueritte-Voegelein F, Lavelle F. Experimental antitumor activity of taxotere (RP 56976, NSC 628503), a taxol analogue. Cancer Res. 1991; 51:4845–4852. [PubMed: 1680023]
33. Andrews NC, Faller DV. A rapid micropreparation technique for extraction of DNA-binding proteins from limiting numbers of mammalian cells. Nucleic Acids Res. 1991; 19:2499. [PubMed: 2041787]
34. Stamey TA, Yang N, Hay AR, McNeal JE, Freiha FS, Redwine E. Prostate-specific antigen as a serum marker for adenocarcinoma of the prostate. N Engl J Med. 1987; 317:909–916. [PubMed: 2442609]

35. Kellokumpu-Lehtinen P, Nurmi M, Koskinen P, Irjala K. Prostate-specific antigen as a marker of adenocarcinoma of prostate. Urol Res. 1989; 17:245–249. [PubMed: 2475959]
36. Liu Y, Denlinger CE, Rundall BK, Smith PW, Jones DR. Suberoylanilide hydroxamic acid induces Akt-mediated phosphorylation of p300, which promotes acetylation and transcriptional activation of RelA/p65. J Biol Chem. 2006; 281:31359–31368. [PubMed: 16926151]
37. Cinar B, Yeung F, Konaka H, Mayo MW, Freeman MR, Zhau HE, Chung LW. Identification of a negative regulatory cis-element in the enhancer core region of the prostate-specific antigen promoter: implications for intersection of androgen receptor and nuclear factor-kappaB signalling in prostate cancer cells. Biochem J. 2004; 379:421–431. [PubMed: 14715080]
38. Palvimo JJ, Reinikainen P, Ikonen T, Kallio PJ, Moilanen A, Janne OA. Mutual transcriptional interference between RelA and androgen receptor. J Biol Chem. 1996; 271:24151–24156. [PubMed: 8798655]
39. Maier JK, Balabanian S, Coffill CR, Stewart A, Pelletier L, Franks DJ, Gendron NH, Mackenzie AE. Distribution of Neuronal Apoptosis Inhibitory Protein in Human Tissues. J Histochem Cytochem. 2007; 55:911–923. [PubMed: 17510375]
40. Poma P, Notarbartolo M, Labbozzetta M, Sanguedolce R, Alaimo A, Carina V, Maurici A, Cusimano A, Cervello M, D'Alessandro N. Antitumor effects of the novel NF-kappaB inhibitor dehydroxymethyl-epoxyquinomicin on human hepatic cancer cells: analysis of synergy with cisplatin and of possible correlation with inhibition of pro-survival genes and IL-6 production. Int J Oncol. 2006; 28:923–930. [PubMed: 16525642]
41. Notarbartolo M, Cervello M, Poma P, Dusonchet L, Meli M, D'Alessandro N. Expression of the IAPs in multidrug resistant tumor cells. Oncol Rep. 2004; 11:133–136. [PubMed: 14654915]
42. Chen Q, Baird SD, Mahadevan M, Besner-Johnston A, Farahani R, Xuan J, Kang X, Lefebvre C, Ikeda JE, Korneluk RG, MacKenzie AE. Sequence of a 131-kb region of 5q13.1 containing the spinal muscular atrophy candidate genes SMN and NAIP. Genomics. 1998; 48:121–127. [PubMed: 9503025]
43. Sandelin A, Wasserman WW, Lenhard B. ConSite: web-based prediction of regulatory elements using cross-species comparison. Nucleic Acids Res. 2004; 32:W249–252. [PubMed: 15215389]
44. Tannock IF, de Wit R, Berry WR, Horti J, Pluzanska A, Chi KN, Oudard S, Theodore C, James ND, Turesson I, Rosenthal MA, Eisenberger MA. Docetaxel plus prednisone or mitoxantrone plus prednisone for advanced prostate cancer. N Engl J Med. 2004; 351:1502–1512. [PubMed: 15470213]
45. Watson RW, Fitzpatrick JM. Targeting apoptosis in prostate cancer: focus on caspases and inhibitors of apoptosis proteins. BJU Int. 2005; 96(Suppl 2):30–34. [PubMed: 16359436]
46. Altieri DC. Survivin, versatile modulation of cell division and apoptosis in cancer. Oncogene. 2003; 22:8581–8589. [PubMed: 14634620]
47. D'Antonio JM, Ma C, Monzon FA, Pflug BR. Longitudinal analysis of androgen deprivation of prostate cancer cells identifies pathways to androgen independence. Prostate. 2008; 68:698–714. [PubMed: 18302219]
48. Romanish MT, Lock WM, van de Lagemaat LN, Dunn CA, Mager DL. Repeated recruitment of LTR retrotransposons as promoters by the anti-apoptotic locus NAIP during mammalian evolution. PLoS Genet. 2007; 3:e10. [PubMed: 17222062]
49. Perkins ND. Post-translational modifications regulating the activity and function of the nuclear factor kappa B pathway. Oncogene. 2006; 25:6717–6730. [PubMed: 17072324]
50. Dziarmaga A, Hueber PA, Iglesias D, Hache N, Jeffs A, Gendron N, Mackenzie A, Eccles M, Goodyer P. Neuronal apoptosis inhibitory protein is expressed in developing kidney and is regulated by PAX2. Am J Physiol. 2006; 291:F913–920.
51. Xu M, Okada T, Sakai H, Miyamoto N, Yanagisawa Y, MacKenzie AE, Hadano S, Ikeda JE. Functional human NAIP promoter transcription regulatory elements for the NAIP and PsiNAIP genes. Biochim Biophys Acta. 2002; 1574:35–50. [PubMed: 11955612]

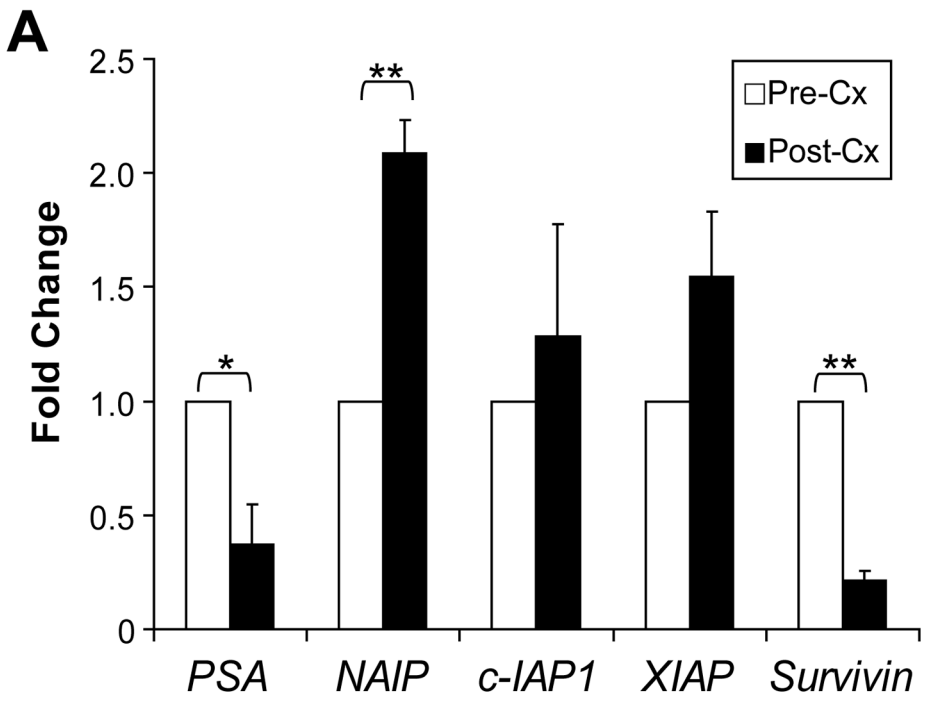

Fig. 1. Levels of IAP mRNA in response to ADT

Levels of mRNA for each gene was normalized to the mRNA levels of *GAPDH* in each biological replicate obtained from the LNCaP hollow fiber model before (pre-Cx) and 10 days after castration (post-Cx). Bars=mean fold-change relative to the pre-castrate levels (1-fold) from three different animals with technical triplicates for each animal. 2-way ANOVA: *, $p \leq 0.05$, **, $p \leq 0.01$.

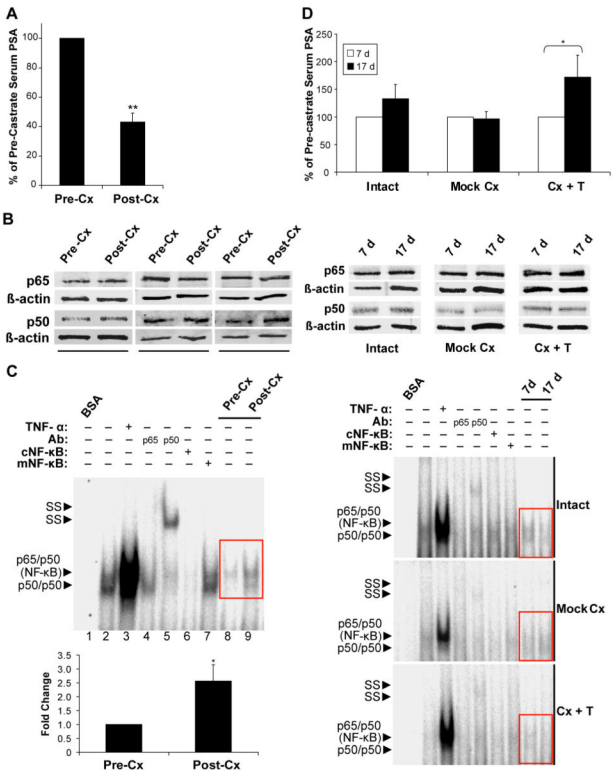

Fig. 2. Expression and DNA-binding activity of NF-κB in response to ADT

A, Serum PSA levels in response to castration were normalized to the number of hollow fibers remaining in the hosts. Pre-castrate levels of PSA were in the range of 14–18 ng/ml and set at 100 % for each host. The bars represent the mean percentages of the pre-castrate serum PSA levels±SD (n=4) before (pre-Cx) and 10 days after castration (post-Cx). *B*, Levels of p65, p50, and β-actin (loading control) proteins in nuclear extracts from cells harvested from the hollow fiber model. Solid bars mark protein extracts from the same animal (n=3). *C*, EMSA using nuclear extracts (5μg protein) obtained from the hollow fiber model from pre-Cx (lane 8) and post-Cx (lane 9) with consensus NF-κB DNA-binding motif. Controls include: BSA (lane 1), nuclear extracts of untreated (lane 2) and TNF-α-stimulated cells (lane 3) that were preincubated with antibodies (Ab) for p65 (lane 4) or p50 (lane 5) or an excess of non-labelled consensus (cNF-κB, lane 6) or mutant (mNF-κB, lane 7) NF-κB oligonucleotides. SS: supershifted antibody-protein-DNA complex. The bands corresponding to the NF-κB (p65/p50)-DNA complex in EMSAs performed using matched samples (pre-Cx and post-Cx) from 3 different animals were quantified using densitometry and presented in bar graph. Solid bars mean fold-change of the biological triplicates of post-Cx compared with the pre-Cx levels (set as 1-fold). *D*, Serum PSA levels, NF-κB expression, and DNA-binding activity were assessed in LNCaP cells obtained from the procedural control mice (n=4 for each set of controls) on 7 days and 17 days after implantation. Intact, no surgical procedure was performed on the mice throughout the experiment; mock Cx, a small incision in the scrotum was made without removal of the testicles 7 days after implantation; Cx+T, a testosterone pellet was added to each mouse upon castration 7 days after implantation of fibers. All images are representative of biological replicates. 2-way ANOVA: *, p≤0.05, **, p≤0.01.

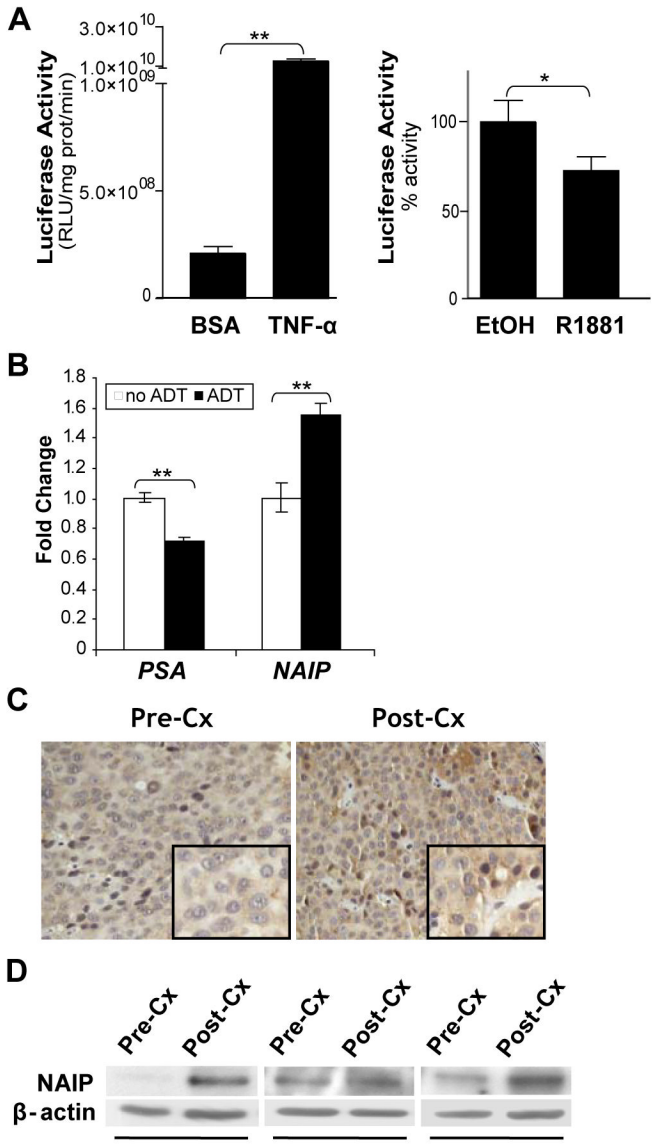

Fig. 3. Androgen status affects transcriptional activity of NF-κB and expression of NAIP

A, NF-κB luciferase reporter gene activity in LNCaP cells treated for 24 hrs with 10ng/ml TNF-α, 10 nM R1881 or SFM with vehicle (BSA for TNF-α treatment and ethanol, EtOH, for R1881 treatment). *B*, Levels of *PSA* and *NAIP* mRNAs measured by qPCR and normalized to levels of GAPDH mRNA in each replicate experiment of cells that were maintained in 10 nM DHT (no ADT) or deprived of androgen (ADT) for 27 hrs. Means±SD are shown (n=3). Student's *t*-test: * P≤0.05, ** P≤0.01. *C*, Representative images of immunohistochemical staining of NAIP expression in LNCaP xenografts obtained from mice before castration (pre-Cx) and 10 days after castration (post-Cx). Magnification, 400 . *D*, levels of NAIP protein detected by western blot analysis using cytosolic extracts (60 μg protein) from cells harvested from the hollow fiber model before (pre-Cx) and 10 days after castration (post-Cx). Bands at 160 kDa corresponded to NAIP protein. The membrane was stripped and reprobed with anti-β-actin (loading control). Solid bars mark protein extracts from the same animal before and after castration (n=3). Images are representative of biological replicates from multiple experiments.

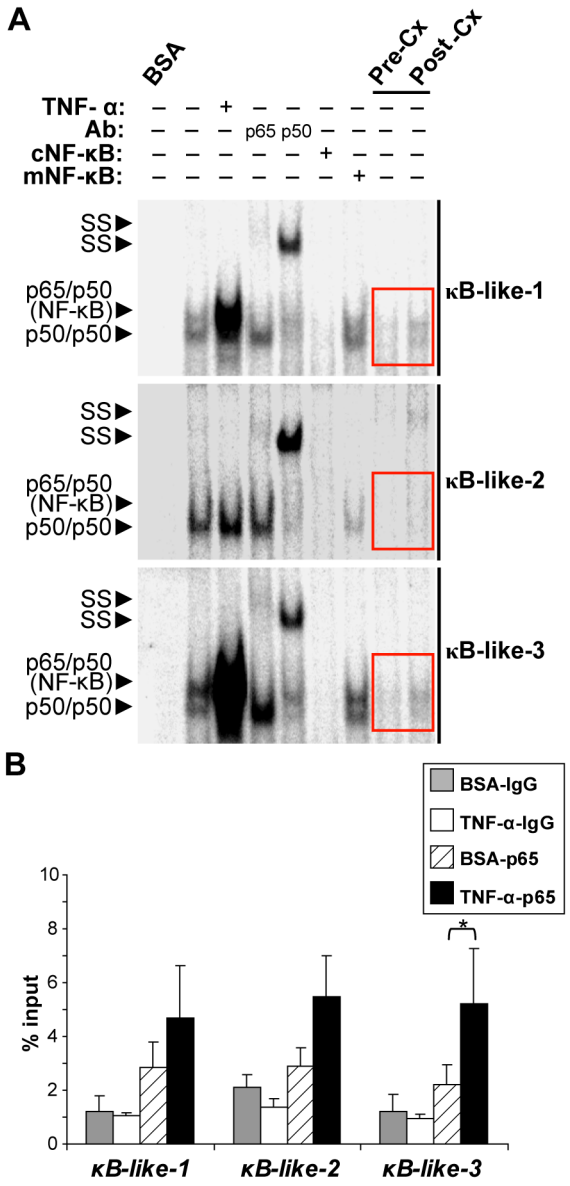

Fig. 4. Recruitment of NF-κB to *NAIP* locus upon ADT

A, NF-κB DNA-binding activity to highly homologous κB sites, κB-like-1, κB-like-2 and κB-like-3 in the *NAIP* locus. Nuclear proteins from untreated LNCaP cells, TNF-α-treated cells and the cells obtained from the *in vivo* hollow fiber models before (pre-Cx) and 10 days after castration (post-Cx) were used for EMSA as described in Fig 2C. *B*, ChIP assay of endogenous NF-κB recruitment to κB-like-1, κB-like-2 and κB-like-3 in the *NAIP* locus in cells treated with 10ng/ml TNF-α (or BSA only as the vehicle control) for 30 min. IP with anti-p65 or IgG (no antibody control). Percentage input of each sample was averaged from triplicates. Student's *t*-test: * p≤0.05, ** p≤0.01. Representative data of biological replicates from multiple experiments are shown.

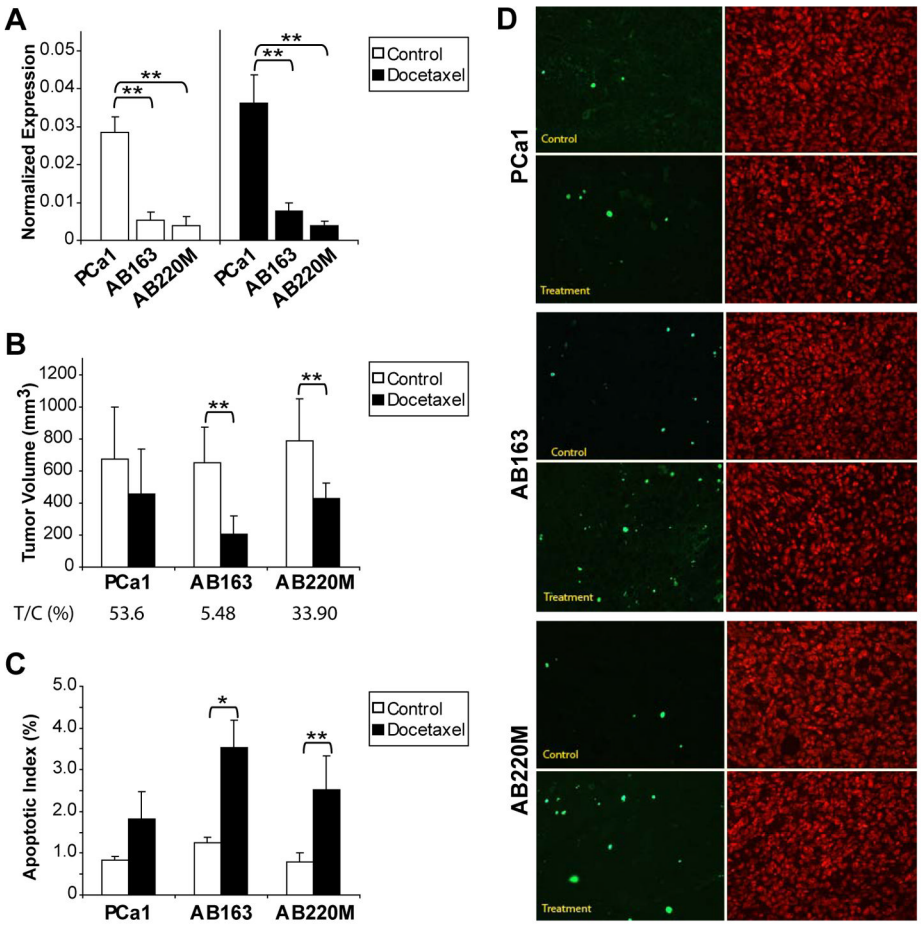

Fig. 5. Elevated levels of NAIP are associated with resistance to chemotherapy and apoptosis

A, Levels of NAIP mRNA normalized to levels of *GAPDH* mRNA in each biological replicate of PCa1, AB163, and AB229M xenografts from animals treated without (control) or with docetaxel. Bars=mean normalized expression from 3 different animals with technical triplicates for each animal. *B*, tumor volume of xenografts at day 20 after grafting. T/C percentage was calculated for each xenograft. *C*, apoptosis evaluated by TUNEL staining. Percentage of apoptotic cells relative to total cells counted in xenografts with or without docetaxel treatment. Approximately 1,400 cells were counted in each xenograft. Bars=means±SD (n>3). 2-way ANOVA: * p≤0.05, ** p≤0.01. *D*, Representative images in four different fields from each xenograft with or without docetaxel treatment. TUNEL (FITC) staining for apoptotic cells in left panels; PI (red) staining for total cells in right panels. Magnification, 40×.

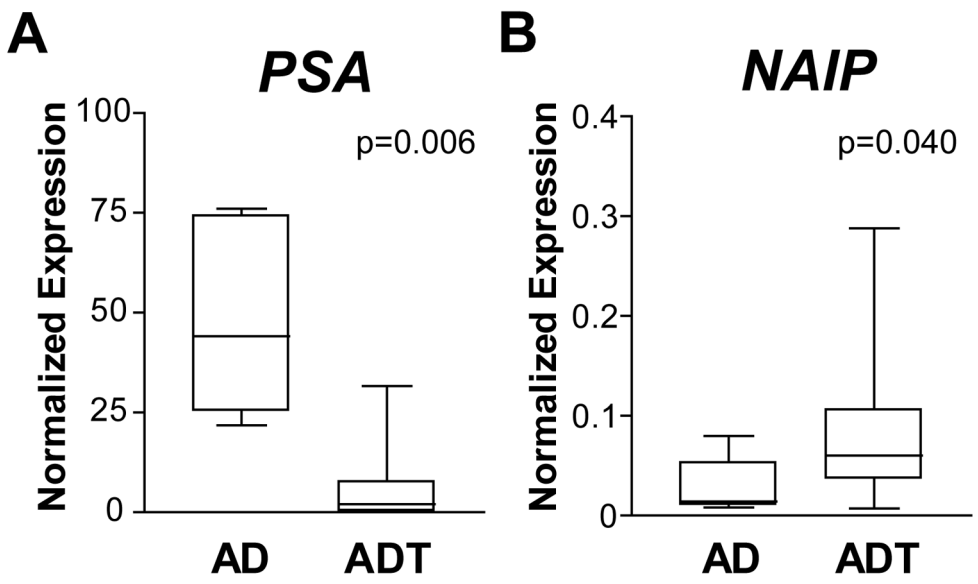

Fig. 6. Levels of NAIP mRNA in clinical CaP tissues

Levels of *PSA* (*A*) and *NAIP* (*B*) mRNA normalized to *GAPDH* mRNA in CaP tissue from men treated with ADT compared to levels in CaP tissue from men not receiving ADT (androgen dependent, AD). Bars=mean normalized expression ± SD. ADT (n=12) and AD (n=6). 2-way ANOVA.

Table 1

NF-κB-binding sites in the *NAIP* promoter and second intron

The sequences and location of κB-like sites in the promoter and second intron of *NAIP*.

Site	* Coordinates	Sequence (5′→3′)	‡ Identity
Concensus		† GGGRNYYYCC	
κB-oligo		GGGACTTTCC	
κB-like-1	−1520 to −1511	GGGGATTTAC	9/10
κB-like-2	−241 to −232	GGGGCTATCC	9/10
κB-like-3	498 to 507bp 5’ to exon 3	GGTAATTTCC	9/10

* Coordinates determined from the sequence are based on GeneBank Accession No. U19251 [42].

† R = any purine, N = any nucleotide, Y = any pyrimidine.

‡ Identity indicates the number of nucleotides which are identical to the 10 nucleotides of the NF-κB consensus sequence.